Communication

Influence of dendritic and equiaxed microstructure of tensile properties variation in AZ91D

Anders E. W. Jarfors[1,] *, Yang Xanjie[2], Hanyi Xia[3], Anshan Yu[4,] and Nils-Erik Andersson[5]

[1] Jönköping University, School of Engineering, Department of Materials and Manufacturing, Box 1026, 551 11 Jönköping, Sweden;anders.jarfors@ju.se

[2] Nanchang University, No.999, Xuefu Avenue, Honggutan New District, Nanchang City, Jiangxi Province, China; yangxj@ncu.edu.cn

[3] Nanchang University, No.999, Xuefu Avenue, Honggutan New District, Nanchang City, Jiangxi Province, China; hyxia1997@163.com

[4] Nanchang University, No.999, Xuefu Avenue, Honggutan New District, Nanchang City, Jiangxi Province, China; yuanshan521521§@163.c0m

[5] Jönköping University, School of Engineering, Department of Materials and Manufacturing, Box 1026, 551 11 Jönköping, Sweden; nils-eric.andersson@ju.se

* Correspondence: anders.jarfors@ju.se

Abstract: There has been controversy around the mechanical properties of Mg-alloys such as AZ91D and the large variation of these have been seen. The current paper addresses this controversy through specially fabricated samples combined with tensile testing and advanced metallography, including 3D reconstruction of the phases. The results show that despite a more brittle nature of the fracture, the equiaxed microstructure displays a better elongation as compared to a dendritic microstructure. The main conclusion is that this is primarily caused by the nature, or tortuosity, of the $Mg_{17}Al_{12}$-network in the material.

Keywords: Mg-alloy; AZ91D; Mechanical properties; Microstructure; Interconnectivity; Metallography; Grain size; Dendrite arm spacing; 3D reconstruction

1. Introduction

The microstructure of AZ91D consists of the primary α-Mg and a divorced eutectic consisting of α-Mg and $Mg_{17}Al_{12}$. In casting, the fraction and morphology of the $Mg_{17}Al_{12}$ phase are dominated by the non-equilibrium solidification kinetics. (1) Morphology and fraction of $Mg_{17}Al_{12}$ are known to have a strong influence on the mechanical properties of AZ91D (2). The formation of an interconnected network of $Mg_{17}Al_{12}$ may be accounted for an improved creep strength of some Mg alloys. (3). The formation of three-dimensional networks of $Mg_{17}Al_{12}$ in High-Pressure Die-Cast (HPDC) AZ91 was also confirmed by Nagasekhar et al. (4). Because of this, it should also be noted that Cáceres et al. (5) stated that there is no meaningful Hall-Petch relationship with grain size effect on the yield stress of HPDC AZ91. Jarfors (6) on the other hand, found a meaningful description for both grain size and Secondary Dendrite Armspacing (SDAS) in AZ91D alloys but not for aluminium. Jarfors (6) attributed this to differences in growth directions in relation to slip plane orientations between FCC and HCP. This does however not explain the difference in finding between Jarfors (6) and Cáceres et al. (5)

Dini et al. (7) discovered another deviation from normal behaviour in AZ91D, through that the yield point displayed a strain rate dependence which could be attributed to the $Mg_{17}Al_{12}$-fraction. The effect of the fraction $Mg_{17}Al_{12}$ on the offset yield strength (Rp0.2) of AZ91D studied further, and

a strong relation to the fraction of $Mg_{17}Al_{12}$ was seen. The main observation was an abrupt increase of Rp0.2 between 9% and 11% $Mg_{17}Al_{12}$ associated with a reduced ductility around 9% $Mg_{17}Al_{12}$.

In work by Dini et al. (7) it was concluded that the formation of $Mg_{17}Al_{12}$ in AZ91D was purely caused by solidification kinetics and solute redistribution following Scheil-type microsegregation. It was furthermore concluded that the $Mg_{17}Al_{12}$-fraction depended on the primary grain size where larger primary grains resulted in higher $Mg_{17}Al_{12}$-fractions. At a grain size of 230μm and a $Mg_{17}Al_{12}$-fraction above 9%, the dependence on grain size became very strong. This suggested that the actual grain configuration has a strong influence on back diffusion and other effects that may influence nucleation and growth of $Mg_{17}Al_{12}$. One more observation was of interest, and that was that the apparent toughness showed a strong, temperature-independent inverse relation to the SDAS. This warrants a deeper investigation of the formation and growth morphology of the $Mg_{17}Al_{12}$ phase and its relationship to mechanical properties.

The current paper aims to take a deeper look at the formation of $Mg_{17}Al_{12}$ and its relationship to the mechanical properties through a study of two extreme cases in the solidification of AZ91D

2. Materials and Methods

The current material was melted under Air and SF6 atmosphere and allowed to solidify in a steel tube. This steel tube with the AZ91D alloy inside was cut to length and re-melted in a Bridgeman furnace under controlled conditions. This allows for a controlled solidification with a well-controlled SDAS. It does not allow for controlled nucleation. The materials will, however, be defect-free and all defects will end up outside the gauge region of the tensile samples to be machined our of these re-solidified rods. The samples were fabricated with two different solidification rates indicated as sample A 6 mm/ s and sample B 0.3 mm/s to force differences in nucleation, growth and segregation.

3.1. Tensile testing

Tensile testing was performed following ASTM-E8, using a Zwick/Roell tensile testing equipment for the two differently processed materials

3.1. Metallographic investigation

The metallographic investigation consisted of three parts, starting with a conventional analysis of the microstructural features of the samples, followed by a fractographic analysis of the material. A 3D reconstruction of the microstructure was also made as the main aim of the paper to understand better the influence of dendrites and the connectivity of the $Mg_{17}Al_{12}$. This was made to understand better the stress-strain behaviour and the link to big differences in elongation to failure.

3.1.1. Longitudinal and transverse sectioning

After tensile testing, samples were taken at the location close to the fracture to obtain the cross-section and longitudinal cross-section of the sample. The sample was metallographically prepared and etched with 4% HNO_3 solution and observed under a light optical microscope.

3.1.2. Fractography

A Fei Quanta 200F environmental scanning electron microscope was used to analyze the surface morphology of the fracture surface of the sample after a tensile fracture. At the same time, EDS was used to collect and analyze the element types and contents in the specified area of the material microstructure.

3.1.1. 3D reconstruction of the microstructure

The metallographic samples were continuously polished and etched; each reconstructed section was 3mm thick. A micro Vickers hardness tester was used to allow positioning and determination of the layer removal thickness, making 3-4 indentations using 300N load. After each polished layer, a two-dimensional image was taken using on a light optical microscope. This process was repeated until 40-50 continuous two-dimensional metallographic images are obtained.

In order to stack and reconstruct the microstructure, each image was checked and filtered to correct and align the images using Photoshop, and the crop the target area. The two-dimensional feature extraction map of the target area is intercepted, and the image is imported into Mimics software for the actual three-dimensional reconstruction.

3. Results and discussion

This section may be divided by subheadings. It should provide a concise and precise description of the experimental results, their interpretation as well as the experimental conclusions that can be drawn.

3.1. Tensile test results

The tensile samples showed very different behaviour with the slowly solidified sample A (0.3mm/s) exhibiting higher strength compared to the rapidly solidified sample B (6mm/s). This is a contradiction to the expected result where a rapidly solidified material should have a refined microstructure and according to a Hall-Petch relationship have a higher yield point. This discrepancy warrants a closer investigation of the cause. The possible causes of this should be in the microstructure either the nucleation is very different, or the amount of secondary phases should differ strongly. The latter was previously suggested by Nagasekhar and co-authors (2,4), as well as suggested by Dini et al. (7). The relationship with grain size and strength is still under debate as illustrated by the differences in findings by Cáceres et al. (5) and by Jarfors (6). To add to the complexity the fact that lower solidification rate leads to larger grains but unexpectedly to higher amounts of $Mg_{17}Al_{12}$-particles leading to possible interconnectivity also adds to the discrepancy that warrants a deeper analysis of the microstructure of these two critical samples and their associated microstructures.

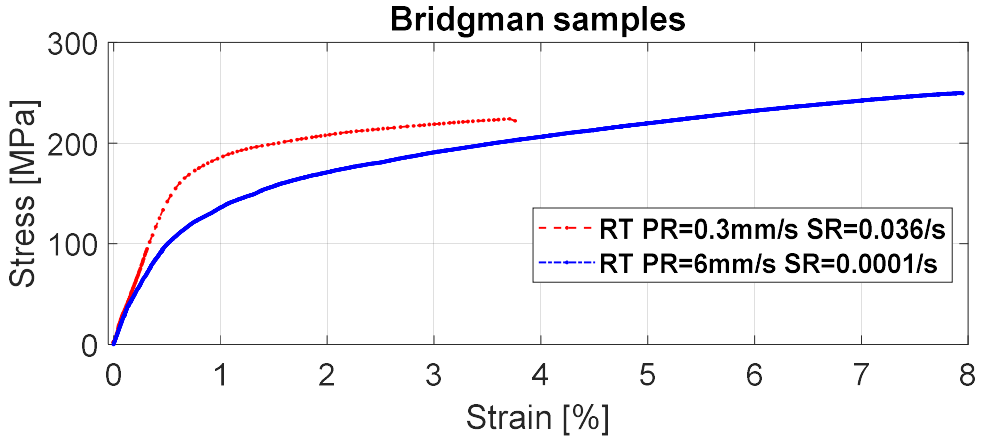

(**a**)

Figure 1. Tensile test results for two Bridgeman solidified samples of AZ 91D with very different stress-strain behaviour.

3.2. Microstructure

The general appearance of the microstructure was characteristics of that of a Bridgeman manufactured microstructure. The main intent was to achieve an equiaxed microstructure in the gauge region of the tensile specimen, but this was difficult for the slowest growth rate of 0.3 mm/s as seen in the longitudinal section, figure 2a. In the transverse direction, figure 2b long secondary arms are also found in the microstructure.

At 6 mm/s the dendritic structure was broken and an equiaxed microstructure was formed, figure 2c and figure 2d for the longitudinal and transverse section respectively. The equiaxed crystals showed the characteristic six arms for growth in the (0001)-plane. Important for the continues discussion is to establish the actual growth along the a-axis in three dimensions for the primary crystal.

Doing a 3D reconstruction of the two different microstructure reveals some interesting features, figure 3a-f. The sample grown at the lower rate, 0.3 mm/s, figure 3a-c, shows on the surface a well-connected and continuous α-Mg phase in the form of dendrites, figure 3a and b. In the longitudinal section, or top view, the $Mg_{17}Al_{12}$-phase appears continuous, but in the perpendicular, to the growth direction, this does not seem to be the case, figure 3a. Looking closer to the details of the $Mg_{17}Al_{12}$-phase, figure 3c, confirms this. The $Mg_{17}Al_{12}$-phase primarily grows along the dendrites creating a strong network, separated by the primary α-Mg dendrite stems. It should be noted that there are contact points in the microstructure where the $Mg_{17}Al_{12}$-phase reaches across to $Mg_{17}Al_{12}$-phase growing along other dendrite stems but these are scarce.

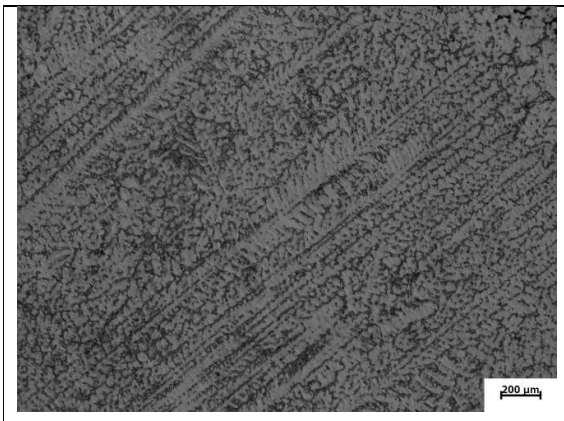

a)

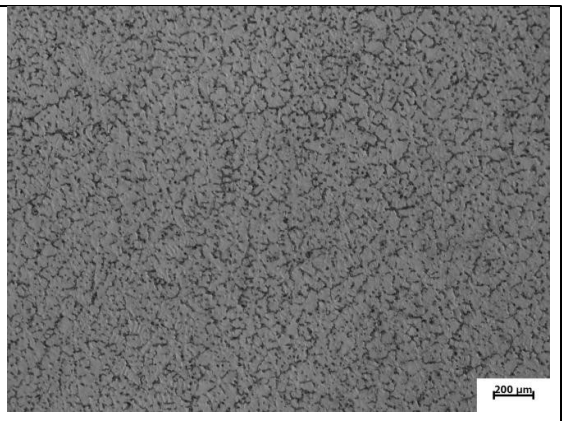

b)

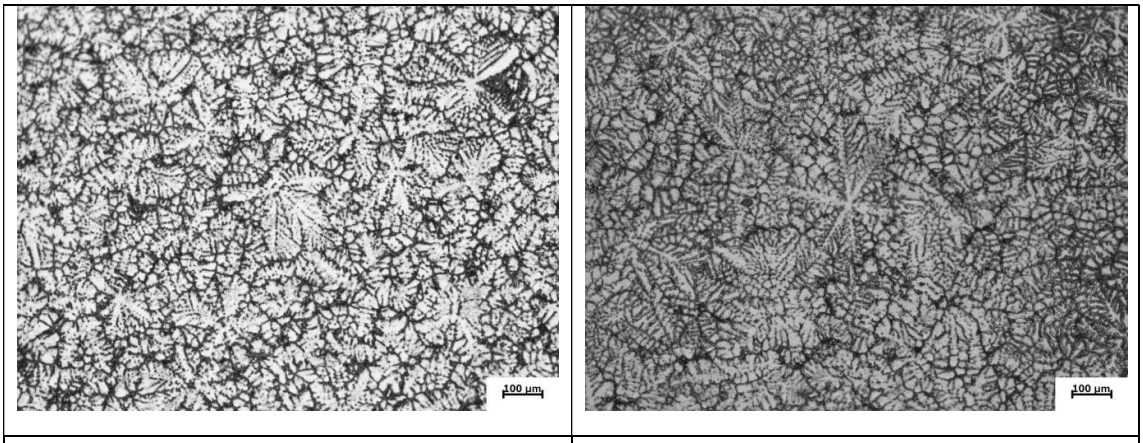

Figure 2. Microstructures of the samples a) Sample grown at 0.3 mm/s longitudinal section b) Sample grown at 0.3 mm/s transverse section, c) Sample grown at 6 mm/s longitudinal section b) Sample grown at 6 mm/s transverse section

Looking closer, the sample grown at the higher rate, 6 mm/s, figure 3d-f, the microstructure of the $Mg_{17}Al_{12}$-phase appears larger but not so well-connected in the top view, figure3d. The primary α-Mg dendritic equiaxed grains does also provide a dense continuous structure, figure 3e, supporting this observation at first glance. Separating the $Mg_{17}Al_{12}$-phase it shows a similar behaviour as in the sample grown at 0.3mm in the sense that it grows along the primary dendrite arms in the equiaxed grains, figure 3f. It does, however, appear as the network can reach across the primary arm, through the network of secondary arms more effectively making the network in the fast grown sample more connected in the grain interior. The $Mg_{17}Al_{12}$-network also appears to connect in the intragranular regions as well and as such, creating a larger and more connected network for the sample grown at 6mm/s, figure 3f. This stresses that the grain size may influence the macroscopic connectivity between the $Mg_{17}Al_{12}$-networks between the grains. It should also be noted that the multitude of dendrite growth directions in the equiaxed structure, figure 3f comparted to the dendritic structure, figure 3c increases the tortuosity of the $Mg_{17}Al_{12}$-networks making it more resilient cracks following the phase boundaries.

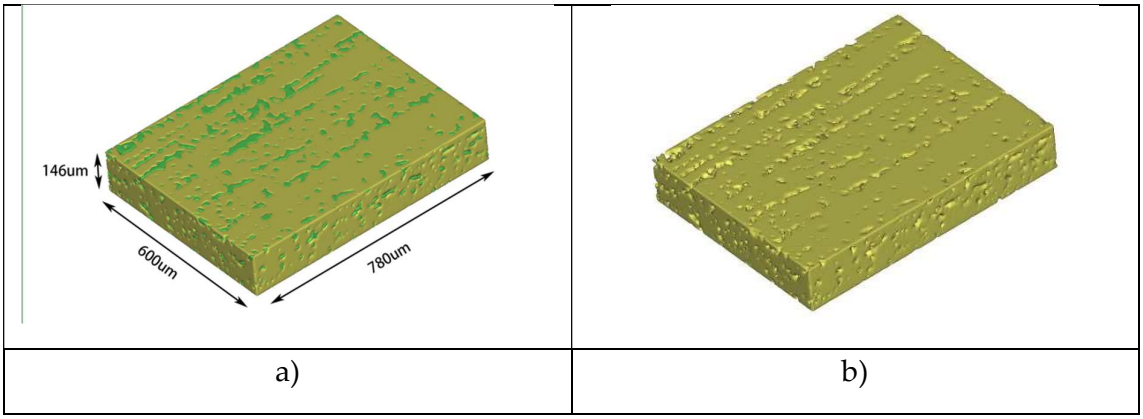

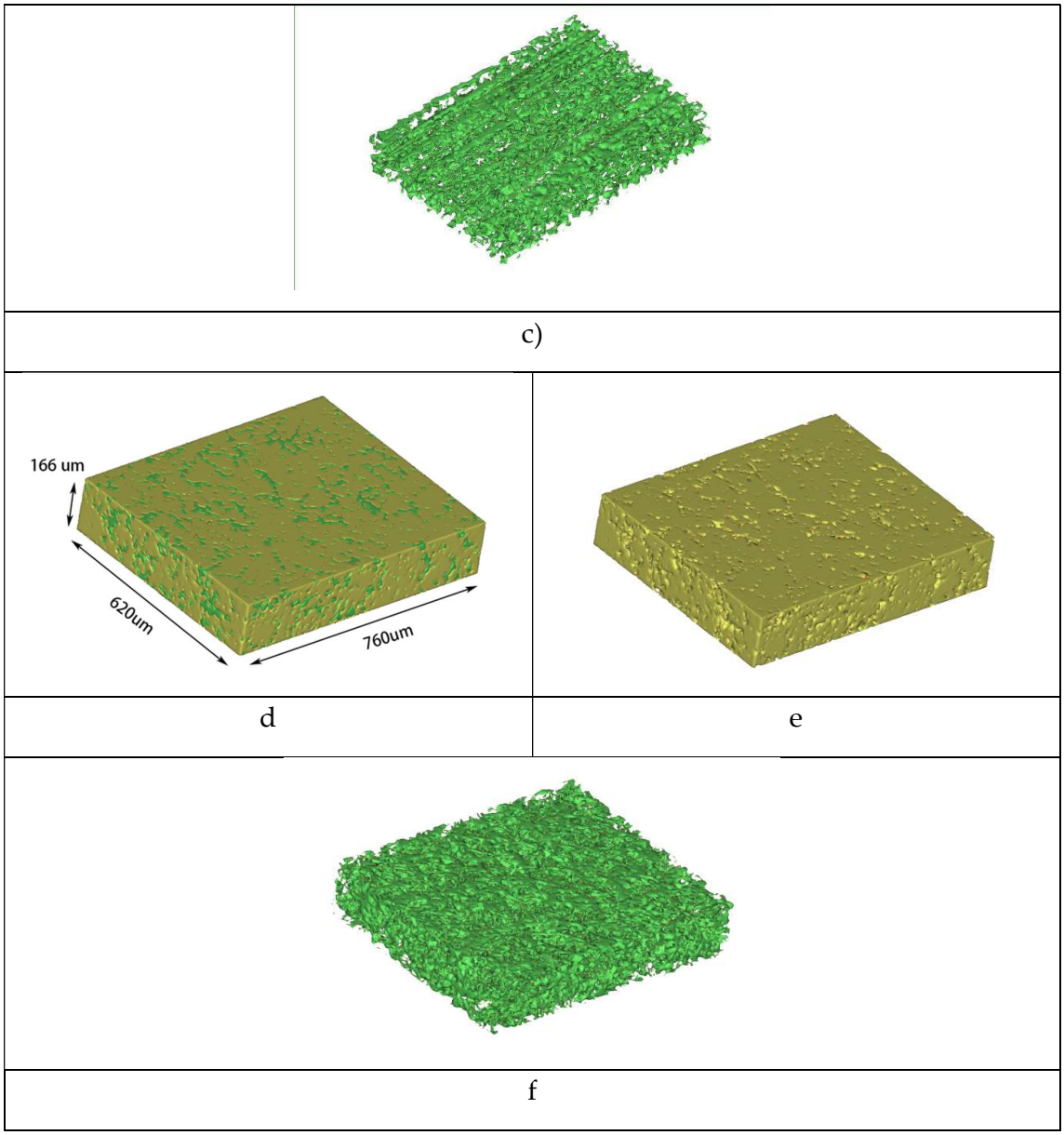

Figure 3. Microstructures of the samples a) Sample grown at 0.3 mm/s complete microstructure b) Sample grown at 0.3 mm/s α-Mg dendrites, c) Sample grown at 0.3mm/s $Mg_{17}Al_{12}$-phase, d) Sample grown at 6 mm/s complete microstructure e) Sample grown at 6 mm/s α-Mg equiaxed dendritic grains, and f) Sample grown at 6 mm/s $Mg_{17}Al_{12}$-phase

3.3. Fractography

The fracture surfaces for both solidification rates displayed a mixed-mode failure with ductile ridges with brittle regions. The fracture for the slowly solidified material appeared somewhat more ductile with ductile ridges spread across the fracture surface, figure 4a compared to the faster-solidified material, figure 4b. The fast-solidified material had regions with angular features and macroscopic steps in the microstructure. This indicated an overall more brittle behaviour on the microscopic scale. This behaviour was not representative for the tensile performance as the sample solidified faster has a lower yield point and a higher elongation to failure than the slowly solidified material. There was thus a contradictive behaviour between the tensile performance and the behaviour of the material on the microscopic level.

The nature of the Mg17Al12-network is the only explanation for the contradiction between the fractography and the actual sample ductility. It appears as if the $Mg_{17}Al_{12}$-phase interface to the α-Mg-phase, represented a weak zone. In the slowly solidified sample A this interface was oriented perpendicular to the tensile stress direction allowing the $Mg_{17}Al_{12}$-network to carry the load, which would explain the higher yield point. Once the $Mg_{17}Al_{12}$-network starts to display cracks, propagation along the $Mg_{17}Al_{12}$/α-Mg interface is easy. For the equiaxed structure, the $Mg_{17}Al_{12}$-network has many orientations, and the weakest link would start to give way earlier. The higher tortuosity will, however, not provide as an energetically beneficial route for the crack propagation. It offers a route both longer and with less energetically beneficial propagation directions, adding to the work of crack propagation. This would then explain the lower strength and the improved elongation despite that the microscopic nature of the cracking is more brittle.

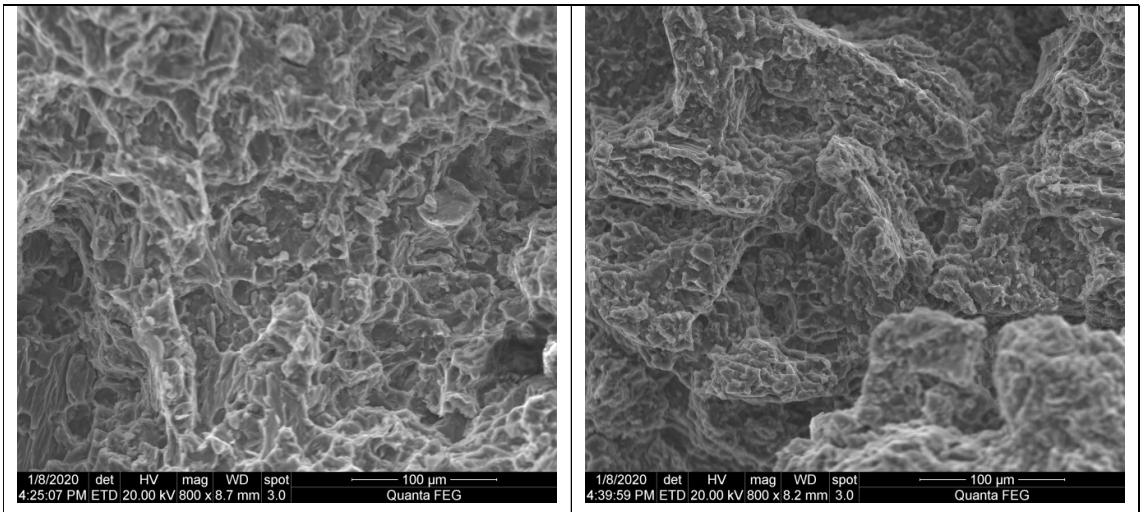

Figure 4. Fracture surfaces of a) Sample A grown at 0.3mm/s, and b) Sample B grown at 6 mm/s.

4. Conclusions

In the current study, the nature of the $Mg_{17}Al_{12}$-phase and its influence on strength and ductility was investigated. The background was the previous findings on the formation of a three-dimensional network $Mg_{17}Al_{12}$ in High-Pressure Die-Cast (HPDC) AZ91D. (3, 4). The nature of the $Mg_{17}Al_{12}$-network has been regarded as one reason for the difficulties to achieve a meaningful Hall-Petch relationship by Cáceres et al. (5), while Jarfors (6) found a meaningful description.

The first important observation in the current study was the apparent contradiction between the fractography and the actual sample ductility, where the more ductile material displays a more brittle nature on the microscopic level. The fractography revealed that the interface $Mg_{17}Al_{12}$/α-Mg was the weak point in the microstructure.

The second observation was that in a larger grain structure, the level of the interconnectivity of the $Mg_{17}Al_{12}$-network was different. The dendrites cause a separation between the $Mg_{17}Al_{12}$-phase regions, and for a finer-grained structure, the interconnectivity was higher. In the current study, this resulted in that a stronger parallel coupling of the properties was the results where the larger grains displayed a higher yield strength. The smaller grains, on the other hand, displayed a lower yield point die to a higher degree of series coupling. The elongation improvement could be explained by a higher tortuosity of the crack path for the fine-grained structure compared to the coarser-grained structure despite a high level of brittle behaviour on the microscopic level.

Author Contributions: Jarfors made conceptualization; methodology devised by Jarfors and Yang; investigation, made by Andersson, Yu and Xia; resources organized by Jarfors and Yang; writing—original draft preparation, Jarfors; writing—review and editing, All authors together; funding acquisition, Jarfors and Yang. All authors have read and agreed to the published version of the manuscript.

Funding: This research was partly funded by the Knowledge Foundation, grant number 20170077.

Acknowledgements: The authors acknowledge Husqvarna AB for supplying the alloy used in the current study.

Conflicts of Interest: The authors declare no conflict of interest. The funders nor material suppliers had any role in the design of the study; in the collection, analyses, or interpretation of data; in the writing of the manuscript, or in the decision to publish the results.

References

1. Prakash DGL, Regener D. Quantitative characterization of Mg17Al12 phase and grain size in HPDC AZ91 magnesium alloy. J Alloys Compd. 2008;461(1–2):139–46.

2. Nagasekhar A V., Caceres CH, Kong C. On the development of a pseudo micro-truss intermetallic microstructure in a high pressure die cast AZ91 alloy. J Phys Conf Ser. 2010;240.

3. Amberger D, Eisenlohr P, Göken M. Microstructural evolution during creep of Ca-containing AZ91. Mater Sci Eng A. 2009;510–511(C):398–402.

4. Nagasekhar A V., Cáceres CH, Kong C. 3D characterization of intermetallics in a high pressure die cast Mg alloy using focused ion beam tomography. Mater Charact [Internet]. 2010;61(11):1035–42. Available from: http://dx.doi.org/10.1016/j.matchar.2010.06.007

5. Cáceres CH, Griffiths JR, Pakdel AR, Davidson CJ. Microhardness mapping and the hardness-yield strength relationship in high-pressure diecast magnesium alloy AZ91. Mater Sci Eng A. 2005;402(1–2):258–68.

6. Jarfors AEW. Grain size and secondary dendrite arm spacing; A priori discussion on the difference between FCC and HCP materials. In: Magnesium Technology 2018. 2018. p. 51–5.

7. Dini H, Andersson N-E, Jarfors AEW. Effects of Microstructure on Deformation Behaviour of AZ91D Cast Alloy. TMS2014 Annu Meet Suppl Proc. 2014;565–72.